Measurement of the ice-nucleating particle concentration using a mobile filter-based sampler on-board of a fixed-wing uncrewed aerial vehicle during the Pallas Cloud Experiment 2022

Alexander Böhmländer¹, Larissa Lacher¹, Kristina Höhler¹, David Brus², Konstantinos-Matthaios Doulgeris², Jessica Girdwood^{3,4}, Thomas Leisner², and Ottmar Möhler¹

Correspondence: Ottmar Möhler (ottmar.moehler@kit.edu)

Abstract. A novel filter-based sampler was deployed during the Pallas Cloud Experiment (PaCE) 2022 for a one-month period in September and October 2022 in Finnish Lapland around 5 km north of the Sammaltunturi station. This area frequently features low-level clouds during autumn. The sampler was deployed on-board of an uncrewed aerial vehicle (UAV) and on the ground. Two filters were deployed simultaneously on the ground and on the UAV to enable a comparison between the two vertical levels. The dataset contains 9 ice-nucleating particle (INP) concentration spectra that feature a temporal overlap at both altitudes, a handling blank filter to assess possible contamination during handling and additional samples from both setups without the temporal overlap. The dataset is the first of its kind, providing altitude-based INP concentrations in Finnish Lapland. There is no clear systematic difference between INP concentrations measured at the different altitudes. The INP concentration is variable over the period measured and also does show some differences on the vertical level. The INP concentration at 253 K varies between $0.15\,l_{\rm std}^{-1}$ and $3.06\,l_{\rm std}^{-1}$ on the ground, and between $0.48\,l_{\rm std}^{-1}$ and $1.69\,l_{\rm std}^{-1}$ at higher altitudes. The connection to synoptic conditions and ambient measurements might provide a better understanding of the origin, lifetime, and distribution of INPs in Finnish Lapland.

1 Introduction

Ice-nucleating particles (INPs) induce the primary ice formation of liquid pure water droplets at supercooled conditions above about -38 °C (e.g., Koop et al., 2000). Mixed-phase clouds (MPCs) exist in the temperature range -38 to 0 °C, where the fraction of ice inside the cloud is controlled by the presence of INP and affects its properties, such as lifetime, radiative budget and precipitation. Precipitation events, and by that the lifetime of a cloud, are linked to the presence of an ice phase in clouds, especially at higher latitudes (e.g., Field and Heymsfield, 2015; Mülmenstädt et al., 2015; Heymsfield et al., 2020). The different radiative properties of MPCs have been investigated in relation to their phase in the literature (e.g., Bellouin et al., 2020; Storelymo, 2017; Shupe and Intrieri, 2004). The nature and sources of atmospheric INPs are understudied, especially

¹Institute of Meteorology and Climate Research, Karlsruhe Institute of Technology, Karlsruhe, Germany

²Atmospheric Composition Research, Finnish Meteorological Institute, Helsinki, Finland

³Centre for Atmospheric and Climate Physics, University of Hertfordshire, Hatfield, Hertfordshire, AL10 9AB, UK

⁴now at: National Centre for Atmospheric Science, School of Earth, Atmospheric and Environmental Sciences, University of Manchester, Manchester, M13 9PL, UK

with a vertical resolution (e.g., Schmale et al., 2021). The vast majority of INP measurements are performed on ground-based stations (e.g., DeMott et al., 2010, 2017; Kanji et al., 2017; Schneider et al., 2020; He et al., 2021). Linking those measurements to upper atmospheric INP concentrations is complicated, since aircraft measurements are expensive and are limited in their altitudes (Shupe et al., 2005; Schmale et al., 2021). In the same way, remote sensing techniques to study aerosol-cloud interactions have to rely on models to estimate certain variables such as the INP concentration (e.g., Dietel et al., 2024). Small and lightweight uncrewed aerial vehicles (UAVs) offer a flexible and cheap method to investigate the lower atmosphere, the reachable vertical extent mostly regulated by power considerations (e.g., Altstädter et al., 2018; Lampert et al., 2020; Marinou et al., 2019; Villa et al., 2016; Yu et al., 2017; Schrod et al., 2017; Bieber et al., 2020; Böhmländer et al., 2024a). This is especially relevant for the Arctic and sub-Arctic regions, where the boundary layer is very shallow and low-level clouds are common (e.g., Shupe et al., 2011; Gierens et al., 2020; Dietel et al., 2024).

This report describes filter-based measurements of atmospheric INP concentrations using a simple and lightweight aerosol sampler technique co-located on the ground and on-board of a fixed-wing uncrewed aerial vehicle (UAV). The sampler consists of a filter holder, a mass flow meter and a small and lightweight multi-diaphragm pump. The flow is monitored during operation to ensure constant operation and detection of failures during flight. The co-location offers the simultaneous INP sampling at the ground and during UAV operation, which enables direct comparison at two different altitudes. The technical description of the setup is detailed in Böhmländer et al. (2024a).

2 Observation site

35

The here described measurements have been done as part of the Pallas Cloud Experiment 2022 (PaCE-2022). The sampling location was around 5 km north of the Sammaltunturi station, which is part of the Pallas Atmosphere-Ecosystem Supersite in Finnish Lapland, hosted by the Finnish Meteorological Institute (FMI) (Asmi et al., 2021; Brus et al., 2024) and part of Global Atmosphere Watch (GAW), Integrated Carbon Observation System (ICOS), European Monitoring and Evaluation Programme (EMEP) and the Aerosol, Clouds and Trace Gases Research Infrastructure (ACTRIS). The Sammaltunturi station is located at 67°58'24" N, 24°60'58" E, while the measurements with the UAV were conducted above an open space (68°1'10" N, 24°8'52" E), indicated in 1. The local vegetation consists of low vascular plants, lichen and moss (e.g., Lohila et al., 2015), while the surrounding forest mainly consists of pine, spruce and birch trees (e.g., Komppula et al., 2005). The anthropogenic impact on the aerosols at the observation site is minor, since it is located inside the Pallas-Yllästunturi National Park and far away from larger settlements (Lohila et al., 2015). The ground setup was located on top of a small hut on an open-field, which was used as a starting and landing area for the UAV. The field is located next to a street with a very low amount of irregular traffic (see also Brus et al., 2024). The goal was to measure at the same time at both altitudes. The altitude for the flight was designated to be just below cloud base to determine the INP concentration close to the cloud. The dataset contains data from the UAV between 405 m and 906 m above mean sea level, resulting in a maximum altitude of 498 m above ground level (agl).

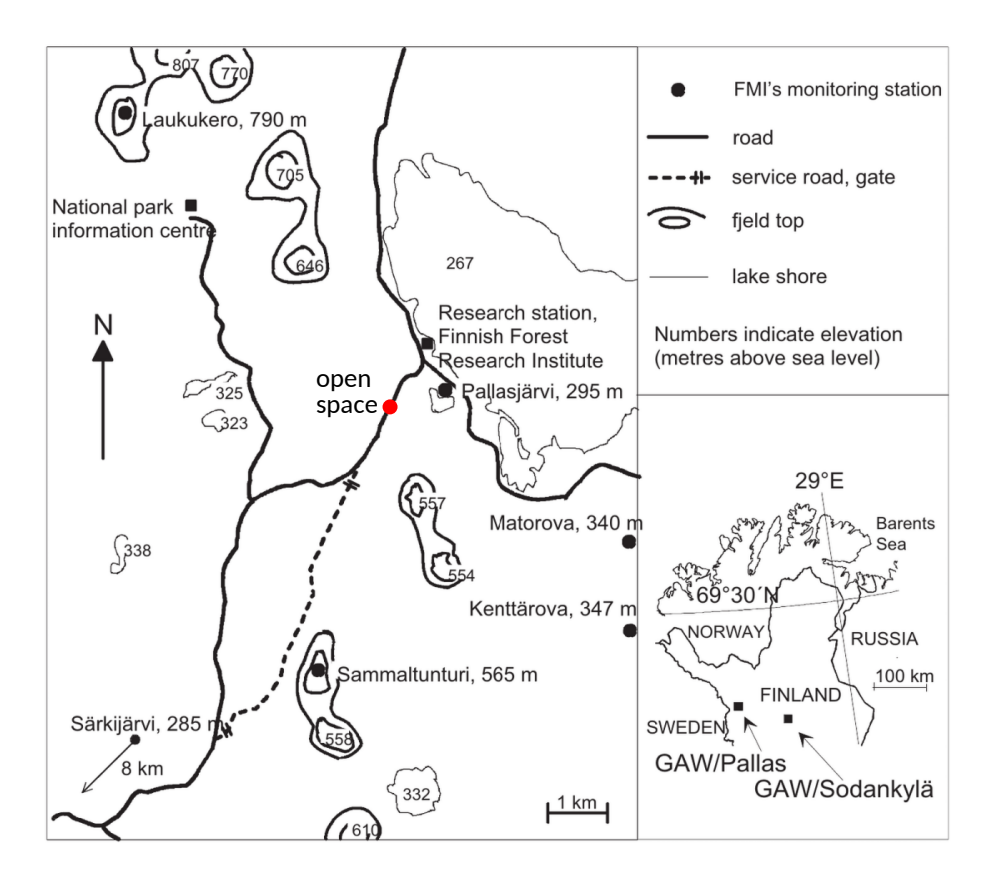


Figure 1. Location of Pallas (lower right) and Sammaltunturi (left). The red dot marks the location of the open space used for the UAV operation during PaCE-2022. Figure adapted from Hatakka et al. (2003).

3 Instrument operation

The filters are placed into the filter holder at a clean working environment, wearing gloves and handling the filters itself only with pre-cleaned forceps. Two filter holders are loaded with a filter each and then sealed with closed off black tubing and stored until deployment inside zip-lock plastic bags. The general filter handling is described in detail in Böhmländer et al. (2024a). All filters were subjected to an active air flow at a constant altitude, during ascend and descent the pump was turned off. For the PaCE-2022 campaign some filters were flown twice, i.e. after a flight, the filter was not switched with a fresh and clean filter, but the same filter was flown a second time under the same conditions. This leads to an enhanced INP concentration sensitivity due to the increase in sampled air-volume. All filters were flown on-board of the Skywalker fixed-wing UAV. The collected filters were stored at room temperature at the site (< 4 weeks) and shipped to KIT, where the filters were stored at -18 °C until analysis with the freezing assay Ice Nucleation Spectrometer of the Karlsruhe Institute of Technology (INSEKT). This instrument consists of an actively cooled aluminium block, which can house two 96-well polymerase chain reaction (PCR) plates. The 192 wells of the two plates were filled with Nanopure water and Nanopure water-based suspensions of the

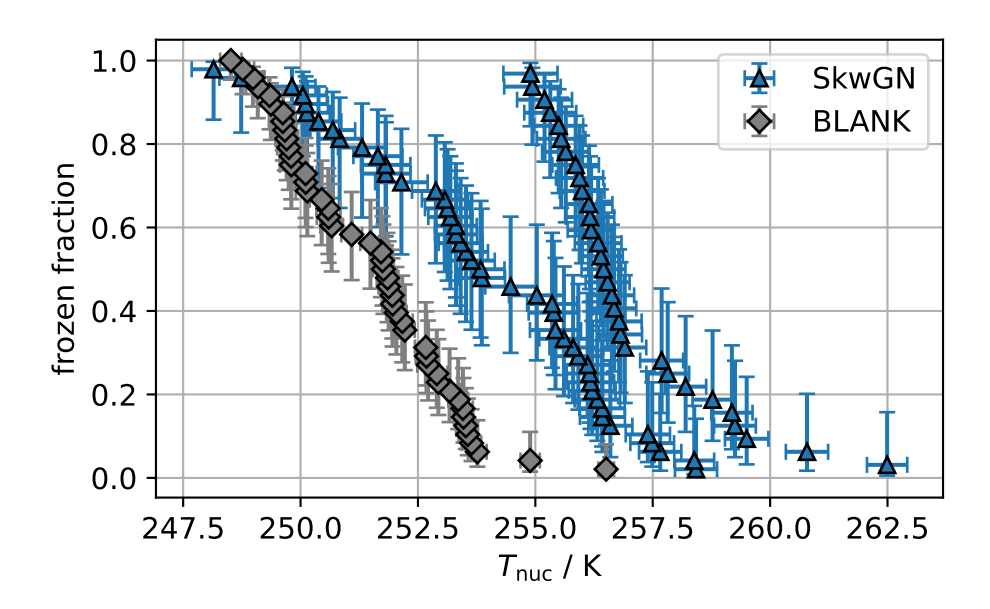


Figure 2. The frozen fraction as a function of the observed freezing temperature $T_{\rm nuc}$ for aerosol particles washed off a ground filter (SkwGN) and off a handling blank filter (BLANK). The two samples from the ground filter are two suspensions with different aerosol concentrations. In this case the left most sample is diluted with dilution factor of 5.

sampled aerosols. The aluminium block houses eight temperature sensors and a camera is located above the sample to detect the brightness of each filled well. The aluminium block and thus the samples in the PCR plates are cooled down at a rate of 0.33 K until all aliquots are frozen. INSEKT is described in detail by Böhmländer et al. (2024a) and references therein.

4 Data evaluation and quality control

The raw data produced by INSEKT contains the data of the eight temperature sensors and the grey scale value of each well derived from the camera output at a frequency of 1 Hz. The freezing temperature is determined by calculating the mean of the temperature sensors as specified in the py_raw_insekt software. The uncertainty of the nucleation temperature is calculated as the standard deviation of the mean, considering a normal distribution. The time when the well freezes is detected by a rapid decrease in the grey scale value. From the amount of frozen droplets in the wells and the total amount of wells filled with the same sample, a frozen fraction is calculated for each sample. Figure 2 shows the frozen fraction of an aerosol sample washed of a loaded filter in comparison to washing water of a handling blank filter taken during the campaign. The uncertainty associated with the frozen fraction is calculated using the normal approximation of the binomial distribution published by Agresti and Coull (1998) assuming a confidence interval of 95 % (see also Hill et al., 2016; Schneider et al., 2020; Böhmländer et al., 2024a). Using the equations established by Vali (1971) the INP concentration per standard litre of sampled air is calculated and shown in Figure 3 for the two different dilutions. Finally, in Figure 4 the information on the different dilutions is removed and a single dataset per filter, describing the INP concentration as a function of the nucleation temperature is shown. This data is given

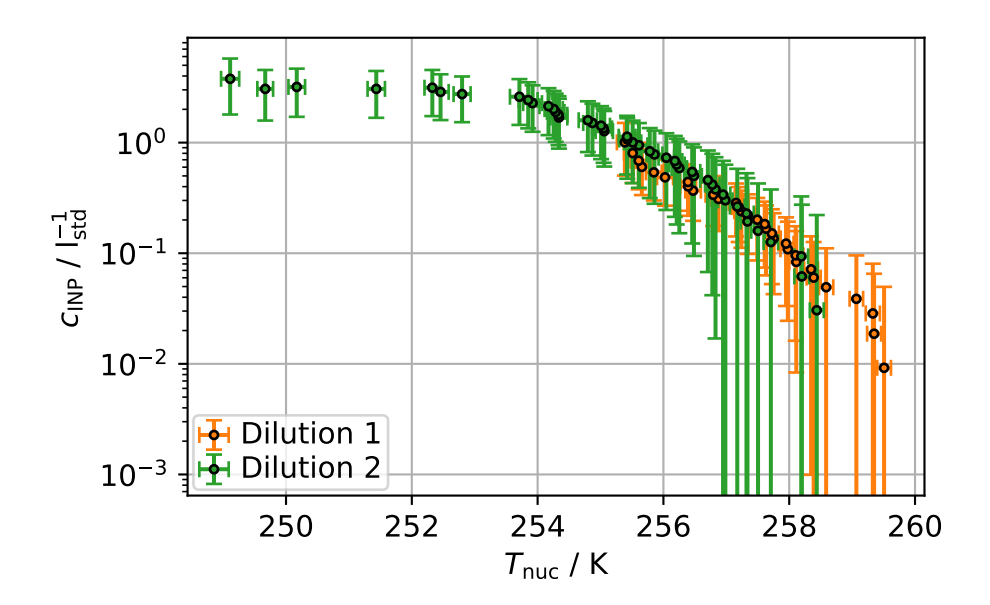


Figure 3. The INP concentration as a function of the freezing temperature $T_{\rm nuc}$. The data is shown for the two suspensions shown in Figure 2.

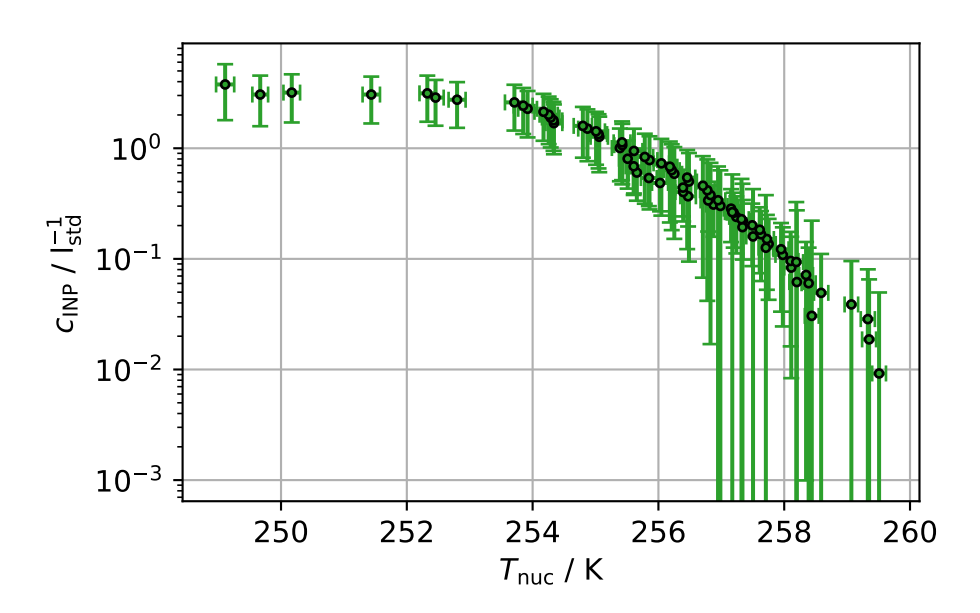


Figure 4. The INP concentration as a function of the freezing temperature $T_{\rm nuc}$ as a homogenized dataset. The two suspensions separately shown in Figure 3 are combined as one for the here presented datasets.

alongside its corresponding frozen fraction for each sample in the dataset presented here. The data is checked considering three potential issues during the analysis with INSEKT, considering three distinctive positions on the frozen fraction scale (0.25, 0.5 and 0.75):

- 1. Quality of the Nanopure water background: the difference between the frozen fraction of the Nanopure water background and the frozen fraction of the given sample should be smaller than 1 K. If this condition is not met, an error flag is associated with the data.
- 2. Separation of suspensions with different aerosol concentrations from the same filter washing water: the difference between the frozen fraction of the suspensions should be smaller than 1 K. If this condition is not met, a warning flag is associated with the data.
- 3. Freezing order: the suspensions should freeze in order, with the one with highest aerosol concentration freezing first. If this condition is not met, an error flag is associated with the data.

Data with error flags are removed from the datasets. Data with warning flags are manually inspected and removed if necessary.

5 Overview of dataset

85

100

The datasets are given as netCDF files following the CF-1.11 metadata conventions. There are three types of datasets provided, differing in their sampling condition. One type of dataset is derived from the aerosol washed of a filter loaded on-board of the UAV (Skw), the other type is from an identical setup on the ground (SkwGN). The third data type is for the handling blank (BLANK), which does not contain any data on the INP concentration, but only on the frozen fraction. Two handling blanks were collected during the campaign, but the data from one of the experiments was corrupted and could not be repeated. The dataset contains pairs of UAV and ground filter samples, which have been sampled during the same time period. Figure 5 shows the comparison between the INP concentration at the ground and at an altitude of 200 m above ground level (agl) sampled on 2022-10-08 09:30:00+0000. The highest INP concentration measured on the ground during this campaign was $13.18^{+6.91}_{-6.53}1^{-1}_{\text{std}}$ ($T_{\text{nuc}} = 252.74 \,\text{K}$), while the highest INP concentration on the UAV was $13.41^{+6.70}_{-6.26}1^{-1}_{\text{std}}$ ($T_{\text{nuc}} = 249.75 \,\text{K}$). The INP concentrations have been measured between 246.92 (247.61) K and 265.38 (266.58) K on the UAV (ground), limited at the lower temperatures by the Nanopure water background and at the higher temperatures by the INP sensitivity of INSEKT. In total, 14 filter samples from UAV flights are available and can be combined with 14 filter samples taken on the ground with a temporal overlap. One additional ground sample and UAV sample are available, but do not have a temporal overlap. The handling blank filter was taken during the campaign and shows the extent of contamination during the handling of the filters. The frozen fraction of all filters as well as of the handling blank is shown in Figure 6. Only one sample shows an overlap with the frozen fraction of the handling blank. The dataset is still included, but should be removed for a future analysis. The frozen fraction of the handling blank is not subtracted from the filter data provided.

110 6 Conclusions

The dataset presented provides the first INP concentration measurements using a mobile filter-based setup utilizing a UAV. The data can be used to assert the INP concentration in the vertical column connecting it to different synoptic conditions. Looking

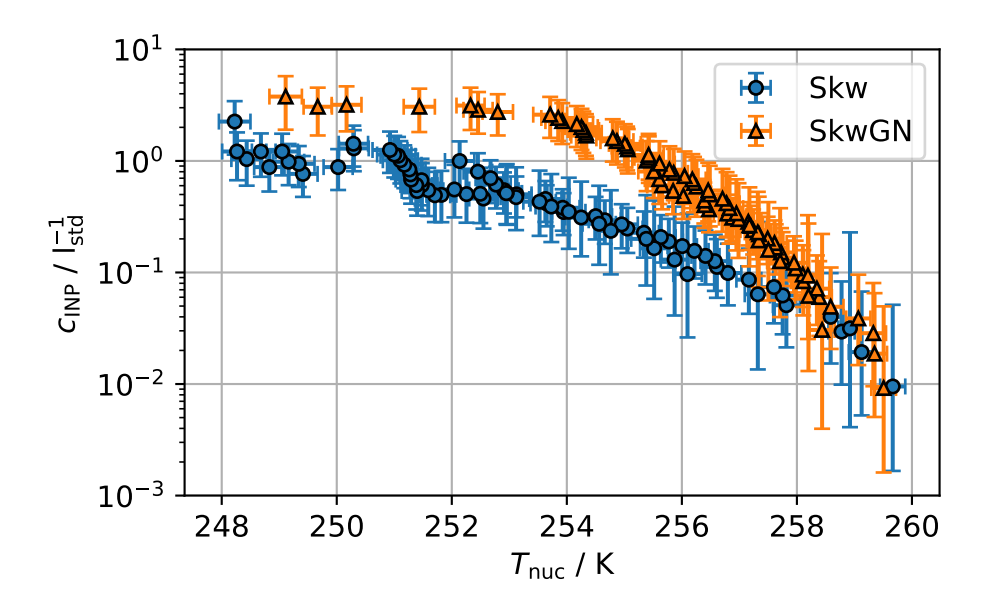


Figure 5. The INP concentration as a function of the observed freezing temperature $T_{\rm nuc}$ for a sample taken on the ground (SkwGN) and on-board of the UAV (Skw).

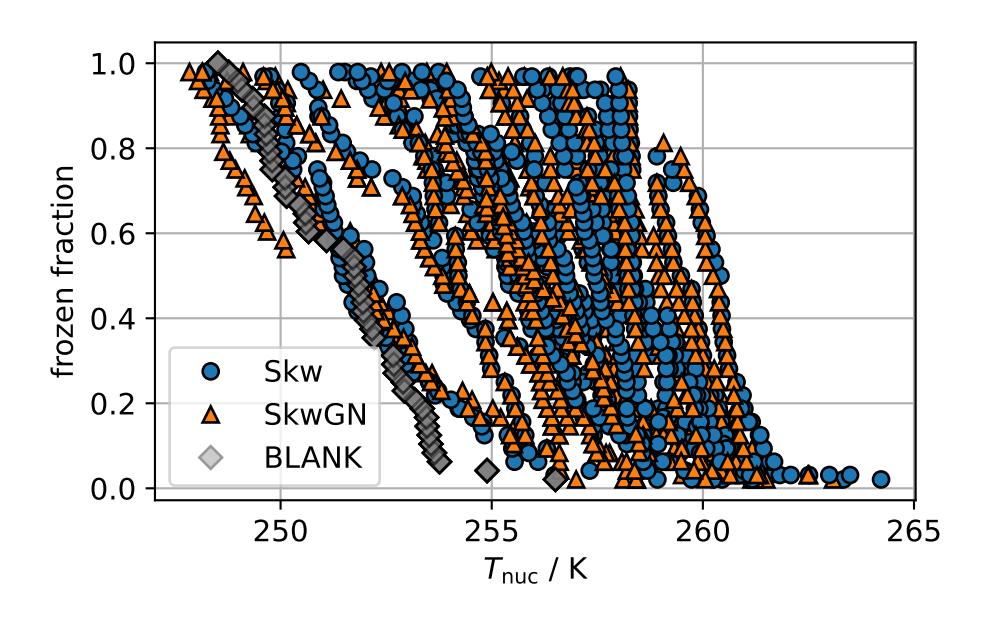


Figure 6. The frozen fraction as a function of the observed freezing temperature $T_{\rm nuc}$ for all filters, split into UAV (Skw), ground (SkwGN) and handling blank (BLANK) samples. Only some diluted samples show a similar frozen fraction as the handling blank. Note that the handling blank suspension is very close to its Nanopure water background.

at individual cloud cases, especially when multiple samples were taken on the same date, offers also a temporal resolution. The Sammaltunturi station, located just 5 km south of the ground measurements, can be used as a reference for other relevant

meteorological variables as well as the measurement of the INP concentration with a high temporal resolution utilizing the Portable Ice Nucleation Experiment (PINE, see also Böhmländer et al., 2025). Since the data is given based on freezing events, the differential spectra can be calculated, obtaining characteristic nucleation temperatures for the aerosol sampled. The measurement of the INP concentration at different verticals levels in the lower atmosphere should be extended in the future. Connecting these measurements with ground-based measurements might prove vital in understanding the impact of INPs on weather and climate via primary ice nucleation in mixed-phase clouds.

7 Code and data availability

Datasets are archived under individual DOI at the Zenodo Open Science data archive (https://doi.org/10.5281/zenodo.16752129, last access: 06082025, Böhmländer et al. (2024b)), where a dedicated community Pallas Cloud Experiment - PaCE2022 has been established (https://zenodo.org/communities/pace2022/, last access: 06082025). This community houses the data files along with additional metadata on the datasets. The py_raw_insekt software is available on a public gitlab instance under https://codebase.helmholtz.cloud/insekt/py_raw_insekt.

Appendix A: Additional information on the filter samples

Table A1 provides additional information on the filter samples collected during PaCE 2022. This information is also available in the metadata of each netCDF file.

130 Author contributions. AB did the data analysis and wrote the manuscript. LL, JG and AB performed the flights during the PaCE-2022 campaign. KH reviewed the original manuscript and provided helpful commentary in later stages. TL developed the LabVIEW software to control and interact with the INSEKT. DB and KD prepared and organized the PaCE-2022 campaign. All authors contributed to the proof reading and discussion of the dataset.

Competing interests. The contact author has declared that none of the authors has any competing interestes.

135 Acknowledgements. This research has been supported by the ACTRIS IMP GA 871115, the ACTRIS-Finland funding through the Ministry of Transport and Communications, and the Atmosphere and Climate Competence Center Flagship funding by the Research Council of Finland (Grants 337552).

The KIT project contribution was supported by the Helmholtz Association through the research program "Changing Earth - Sustaining our Future". The authors would like to thank the technical team at the Sammaltunturi station for their support during the campaign, and the INSEKT team at KIT for continuous support in developing and operating INSEKT.

Table A1. Additional information on the experiments. The total volume of air is given in standard liters with the reference of $T = 273.15 \,\mathrm{K}$ and $p = 101325 \,\mathrm{Pa}$ and calculated from the total flight time and the mean flow.

Total volume of air / $l_{\rm std}$	Filename	start time (UTC+3)	stop time (UTC+3)
1950	KIT.SkwGN.b1.20220929.1049.nc	2022-09-29 13:49:00	2022-09-29 16:45:00
1352	KIT.Skw.b1.20220930.0943.nc	2022-09-30 12:43:00	2022-09-30 14:56:00
1420	KIT.SkwGN.b1.20220930.0943.nc	2022-09-30 12:43:00	2022-09-30 14:56:00
1550	KIT.Skw.b1.20221001.1055.nc	2022-10-01 13:55:00	2022-10-01 16:31:00
1719	KIT.SkwGN.b1.20221001.1055.nc	2022-10-01 13:55:00	2022-10-01 16:31:00
451	KIT.SkwGN.b1.20221001.1459.nc	2022-10-01 17:59:00	2022-10-01 18:35:00
258	KIT.Skw.b1.20221005.1041.nc	2022-10-05 13:41:00	2022-10-05 14:03:00
3979	KIT.SkwGN.b1.20221005.1041.nc	2022-10-05 13:41:00	2022-10-05 19:27:00
184	KIT.Skw.b1.20221006.1431.nc	2022-10-06 17:31:00	2022-10-06 17:47:00
2857	KIT.SkwGN.b1.20221006.1431.nc	2022-10-06 17:31:00	2022-10-06 21:27:00
534	KIT.Skw.b1.20221008.0930.nc	2022-10-08 12:30:00	2022-10-08 13:28:00
552	KIT.SkwGN.b1.20221008.0930.nc	2022-10-08 12:30:00	2022-10-08 13:28:00
708	KIT.Skw.b1.20221008.1231.nc	2022-10-08 15:31:00	2022-10-08 16:48:00
744	KIT.SkwGN.b1.20221008.1231.nc	2022-10-08 15:31:00	2022-10-08 16:48:00
960	KIT.Skw.b1.20221010.0915.nc	2022-10-10 12:15:00	2022-10-10 13:50:00
1007	KIT.SkwGN.b1.20221010.0915.nc	2022-10-10 12:15:00	2022-10-10 13:50:00
1145	KIT.Skw.b1.20221010.1316.nc	2022-10-10 16:16:00	2022-10-10 18:07:00
1096	KIT.Skw.b1.20221011.0948.nc	2022-10-11 12:48:00	2022-10-11 14:39:00
1133	KIT.SkwGN.b1.20221011.0948.nc	2022-10-11 12:48:00	2022-10-11 14:39:00
677	KIT.Skw.b1.20221011.1356.nc	2022-10-11 16:56:00	2022-10-11 17:55:00
718	KIT.SkwGN.b1.20221011.1356.nc	2022-10-11 16:56:00	2022-10-11 17:55:00
915	KIT.SkwGN.b1.20221014.1341.nc	2022-10-14 16:41:00	2022-10-14 17:54:00

The handling blank filter is not shown since no active air flow passed over the filter.

References

Agresti, A. and Coull, B. A.: Approximate is Better than "Exact" for Interval Estimation of Binomial Proportions, The American Statistician, 52, 119–126, https://doi.org/10.1080/00031305.1998.10480550, 1998.

Altstädter, B., Platis, A., Jähn, M., Baars, H., Lückerath, J., Held, A., Lampert, A., Bange, J., Hermann, M., and Wehner, B.: Airborne observations of newly formed boundary layer aerosol particles under cloudy conditions, Atmospheric Chemistry and Physics, 18, 8249–8264, https://doi.org/10.5194/acp-18-8249-2018, 2018.

Asmi, E., Backman, J., Servomaa, H., Virkkula, A., Gini, M. I., Eleftheriadis, K., Müller, T., Ohata, S., Kondo, Y., and Hyvärinen, A.: Absorption instruments inter-comparison campaign at the Arctic Pallas station, Atmospheric Measurement Techniques, 14, 5397–5413, https://doi.org/10.5194/amt-14-5397-2021, 2021.

- Bellouin, N., Quaas, J., Gryspeerdt, E., Kinne, S., Stier, P., Watson-Parris, D., Boucher, O., Carslaw, K. S., Christensen, M., Daniau, A.-L., Dufresne, J.-L., Feingold, G., Fiedler, S., Forster, P., Gettelman, A., Haywood, J. M., Lohmann, U., Malavelle, F., Mauritsen, T., McCoy, D. T., Myhre, G., Mülmenstädt, J., Neubauer, D., Possner, A., Rugenstein, M., Sato, Y., Schulz, M., Schwartz, S. E., Sourdeval, O., Storelvmo, T., Toll, V., Winker, D., and Stevens, B.: Bounding Global Aerosol Radiative Forcing of Climate Change, Reviews of Geophysics, 58, https://doi.org/10.1029/2019rg000660, 2020.
- Bieber, P., Seifried, T. M., Burkart, J., Gratzl, J., Kasper-Giebl, A., Schmale, D. G., and Grothe, H.: A Drone-Based Bioaerosol Sampling System to Monitor Ice Nucleation Particles in the Lower Atmosphere, Remote Sensing, 12, 552, https://doi.org/10.3390/rs12030552, 2020.
 - Brus, D., Doulgeris, K.-M., Bagheri, G., Bodenschatz, E., Pohorsky, R., Schmale, J., Böhmländer, A., Möhler, O., Lacher, L., Girdwood, J., Gratzl, J. G., Kaikkonen, V., O'Connor, E., Le, V., Backman, J., and Servomaa, H.: Data generated during the Pallas Cloud Experiment 2022 campaign: an introduction and overview, Earth System Science Data, in preparation for this SI of ESSD, 2024.

160

175

- Böhmländer, A., Lacher, L., Fösig, R., Büttner, N., Nadolny, J., Brus, D., Doulgeris, K.-M., and Möhler, O.: Measurement of the ice-nucleating particle concentration with the Portable Ice Nucleation Experiment during the Pallas Cloud Experiment 2022, Earth System Science Data, in preparation for this SI of ESSD, 2025.
- Böhmländer, A. J., Lacher, L., Brus, D., Doulgeris, K.-M., Brasseur, Z., Boyer, M., Kuula, J., Leisner, T., and Möhler, O.: A novel aerosol filter sampler for measuring the vertical distribution of ice-nucleating particles via fixed-wing uncrewed aerial vehicles, https://doi.org/10.5194/amt-2024-120, 2024a.
 - Böhmländer, A. J., Lacher, L., and Möhler, O.: Data from filter-based sampler from the ground and on-board of an uncrewed aerial vehicle during the Pallas Cloud Experiment 2022 [data set], https://doi.org/10.5281/zenodo.13911633, 2024b.
- DeMott, P. J., Prenni, A. J., Liu, X., Kreidenweis, S. M., Petters, M. D., Twohy, C. H., Richardson, M. S., Eidhammer, T., and Rogers, D. C.:
 Predicting global atmospheric ice nuclei distributions and their impacts on climate, Proceedings of the National Academy of Sciences,
 107, 11 217–11 222, https://doi.org/10.1073/pnas.0910818107, 2010.
 - DeMott, P. J., Hill, T. C. J., Petters, M. D., Bertram, A. K., Tobo, Y., Mason, R. H., Suski, K. J., McCluskey, C. S., Levin, E. J. T., Schill, G. P., Boose, Y., Rauker, A. M., Miller, A. J., Zaragoza, J., Rocci, K., Rothfuss, N. E., Taylor, H. P., Hader, J. D., Chou, C., Huffman, J. A., Pöschl, U., Prenni, A. J., and Kreidenweis, S. M.: Comparative measurements of ambient atmospheric concentrations of ice nucleating particles using multiple immersion freezing methods and a continuous flow diffusion chamber, Atmos. Chem. Phys., 17, 11 227–11 245, https://doi.org/10.5194/acp-17-11227-2017, 2017.
 - Dietel, B., Sourdeval, O., and Hoose, C.: Characterisation of low-base and mid-base clouds and their thermodynamic phase over the Southern Ocean and Arctic marine regions, Atmospheric Chemistry and Physics, 24, 7359–7383, https://doi.org/10.5194/acp-24-7359-2024, 2024.
- Field, P. R. and Heymsfield, A. J.: Importance of snow to global precipitation, Geophysical Research Letters, 42, 9512–9520, https://doi.org/10.1002/2015gl065497, 2015.
 - Gierens, R., Kneifel, S., Shupe, M. D., Ebell, K., Maturilli, M., and Löhnert, U.: Low-level mixed-phase clouds in a complex Arctic environment, Atmospheric Chemistry and Physics, 20, 3459–3481, https://doi.org/10.5194/acp-20-3459-2020, publisher: Copernicus GmbH, 2020.
- Hatakka, J., Aalto, T., Aaltonen, V., Aurela, M., Hakola, H., Komppula, M., Laurila, T., Lihavainen, H., Paatero, J., Salminen, K., and Viisanen, Y.: Overview of the atmospheric research activities and results at Pallas GAW station, Boreal Environment Research, 8, 2003.
 - He, C., Yin, Y., Wang, W., Chen, K., Mai, R., Jiang, H., Zhang, X., and Fang, C.: Aircraft observations of ice nucleating particles over the Northern China Plain: Two cases studies, Atmospheric Research, 248, 105 242, https://doi.org/10.1016/j.atmosres.2020.105242, 2021.

- Heymsfield, A. J., Schmitt, C., Chen, C.-C.-J., Bansemer, A., Gettelman, A., Field, P. R., and Liu, C.: Contributions of the Liquid and Ice Phases to Global Surface Precipitation: Observations and Global Climate Modeling, Journal of the Atmospheric Sciences, 77, 2629–2648, https://doi.org/10.1175/jas-d-19-0352.1, 2020.
 - Hill, T. C. J., DeMott, P. J., Tobo, Y., Fröhlich-Nowoisky, J., Moffett, B. F., Franc, G. D., and Kreidenweis, S. M.: Sources of organic ice nucleating particles in soils, Atmospheric Chemistry and Physics, 16, 7195–7211, https://doi.org/10.5194/acp-2016-1, 2016.
 - Kanji, Z. A., Ladino, L. A., Wex, H., Boose, Y., Burkert-Kohn, M., Cziczo, D. J., and Krämer, M.: Overview of Ice Nucleating Particles, Meteorological Monographs, 58, 11–133, https://doi.org/10.1175/amsmonographs-d-16-0006.1, 2017.
- Komppula, M., Lihavainen, H., Kerminen, V., Kulmala, M., and Viisanen, Y.: Measurements of cloud droplet activation of aerosol particles at a clean subarctic background site, Journal of Geophysical Research: Atmospheres, 110, https://doi.org/10.1029/2004jd005200, 2005.
 - Koop, T., Luo, B., Tsias, A., and Peter, T.: Water activity as the determinant for homogeneous ice nucleation in aqueous solutions, Nature, 406, 611–614, https://doi.org/10.1038/35020537, 2000.
- Lampert, A., Altstädter, B., Bärfuss, K., Bretschneider, L., Sandgaard, J., Michaelis, J., Lobitz, L., Asmussen, M., Damm, E., Käthner, R., Krüger, T., Lüpkes, C., Nowak, S., Peuker, A., Rausch, T., Reiser, F., Scholtz, A., Sotomayor Zakharov, D., Gaus, D., Bansmer, S., Wehner, B., and Pätzold, F.: Unmanned Aerial Systems for Investigating the Polar Atmospheric Boundary Layer—Technical Challenges and Examples of Applications, Atmosphere, 11, https://doi.org/10.3390/atmos11040416, 2020.
- Lohila, A., Penttilä, T., Jortikka, S., Aalto, T., Anttila, P., Asmi, E., Aurela, M., Hatakka, J., Hellén, H., Henttonen, H., Hänninen, P., Kilkki, J., Kyllönen, K., Laurila, T., Lepistö, A., Lihavainen, H., Makkonen, U., Paatero, J., Rask, M., Sutinen, R., Tuovinen, J.-P., Vuorenmaa, J., and Viisanen, Y.: Preface to the special issue on integrated research of atmosphere, ecosystems and environment at Pallas, in: Boreal Environment Research, vol. 20, pp. 431–454, 2015.
 - Marinou, E., Tesche, M., Nenes, A., Ansmann, A., Schrod, J., Mamali, D., Tsekeri, A., Pikridas, M., Baars, H., Engelmann, R., Voudouri, K. A., Solomos, S., Sciare, J., Groß, S., Ewald, F., and Amiridis, V.: Retrieval of ice-nucleating particle concentrations from lidar observations and comparison with UAV in situ measurements, Atmos. Chem. Phys., 19, 11315–11342, https://doi.org/10.5194/acp-19-11315-2019, 2019.
 - Mülmenstädt, J., Sourdeval, O., Delanoë, J., and Quaas, J.: Frequency of occurrence of rain from liquid-, mixed-, and ice-phase clouds derived from A-Train satellite retrievals, Geophys. Res. Lett., 42, 6502–6509, https://doi.org/10.1002/2015GL064604, 2015.

210

- Schmale, J., Zieger, P., and Ekman, A. M. L.: Aerosols in current and future Arctic climate, Nature Climate Change, 11, 95–105, https://doi.org/10.1038/s41558-020-00969-5, 2021.
- Schneider, J., Höhler, K., Heikkilä, P., Keskinen, J., Bertozzi, B., Bogert, P., Schorr, T., Umo, N. S., Vogel, F., Brasseur, Z., Wu, Y., Hakala, S., Duplissy, J., Moisseev, D., Kulmala, M., Adams, M. P., Murray, B. J., Korhonen, K., Hao, L., Thomson, E. S., Castarède, D., Leisner, T., Petäjä, T., and Möhler, O.: The seasonal cycle of ice-nucleating particles linked to the abundance of biogenic aerosol in boreal forests, Atmospheric Chemistry and Physics, 21, 3899–3918, https://doi.org/10.5194/acp-2020-683, 2020.
- Schrod, J., Weber, D., Drücke, J., Keleshis, C., Pikridas, M., Ebert, M., Cvetkovic, B., Nickovic, S., Marinou, E., Baars, H., Ansmann, A.,

 Vrekoussis, M., Mihalopoulos, N., Sciare, J., Curtius, J., and Bingemer, H. G.: Ice nucleating particles over the Eastern Mediterranean measured by unmanned aircraft systems, Atmos. Chem. Phys., 17, 4817–4835, https://doi.org/10.5194/acp-17-4817-2017, 2017.
 - Shupe, M. D. and Intrieri, J. M.: Cloud Radiative Forcing of the Arctic Surface: The Influence of Cloud Properties, Surface Albedo, and Solar Zenith Angle, Journal of Climate, 17, 616–628, https://doi.org/10.1175/1520-0442(2004)017<0616:crfota>2.0.co;2, 2004.
- Shupe, M. D., Uttal, T., and Matrosov, S. Y.: Arctic Cloud Microphysics Retrievals from Surface-Based Remote Sensors at SHEBA, Journal of Applied Meteorology, 44, 1544–1562, https://doi.org/10.1175/jam2297.1, 2005.

- Shupe, M. D., Walden, V. P., Eloranta, E., Uttal, T., Campbell, J. R., Starkweather, S. M., and Shiobara, M.: Clouds at Arctic Atmospheric Observatories. Part I: Occurrence and Macrophysical Properties, Journal of Applied Meteorology and Climatology, 50, 626–644, https://doi.org/10.1175/2010jamc2467.1, 2011.
- Storelvmo, T.: Aerosol Effects on Climate via Mixed-Phase and Ice Clouds, Annual Review of Earth and Planetary Sciences, 45, 199–222, https://doi.org/10.1146/annurev-earth-060115-012240, 2017.
 - Vali, G.: Quantitative Evaluation of Experimental Results and the Heterogeneous Freezing Nucleation of Supercooled Liquids, J. Atmos. Sci., 28, 402–409, https://doi.org/10.1175/1520-0469(1971)028<0402:qeoera>2.0.co;2, 1971.
 - Villa, T., Gonzalez, F., Miljievic, B., Ristovski, Z., and Morawska, L.: An Overview of Small Unmanned Aerial Vehicles for Air Quality Measurements: Present Applications and Future Prospectives, Sensors, 16, 1072, https://doi.org/10.3390/s16071072, 2016.
- 235 Yu, F., Liu, Y., Fan, L., Li, L., Han, Y., and Chen, G.: Design and implementation of atmospheric multi-parameter sensor for UAV-based aerosol distribution detection, Sensor Review, 37, 196–210, https://doi.org/10.1108/sr-09-2016-0199, 2017.